Helicates of Chiragen-Type Ligands and Their Aptitude for Chiral Self-Recognition

Olimpia Mamula,[a, b] Alex von Zelewsky,*[a] Pierre Brodard,[a] Carl-Wilhelm Schläpfer,[a] Gérald Bernardinelli,[c] and Helen Stoeckli-Evans[d]

Abstract: Two (−)-5,6-pinene-bipyridine moieties connected by a *para*-xylylene bridge (so-called chiragen-type ligands), (−)-L1, undergo self-assembly upon reaction with equimolar amounts of Cu^{I} to form enantiopure circular hexanuclear *P*-helicates. If both enantiomers of L1 are used, mixtures of *P* and *M* hexanuclear helicates are exclusively obtained through a complete chiral recognition; that is, no mixing of the (+) and (−) ligands, respectively, occurs upon complexation. This was proven by a) NMR spectroscopy where identical spectra to those for complexes with the enantiomerically pure ligands were obtained and b) circular dichroism (CD) spectroscopy. The reaction is completely changed by the use of the corresponding *meso*-L1. Instead of well-defined species, oligomeric mixtures are observed, a result demonstrating the crucial role played by ligand chirality in self-assembly processes. Structural variations on the chiral ligand L1, such as a *meta*-xylylene bridge instead of a *para*-xylylene one (in L4) or four pinene groups instead of two (in L5 and L6), favor non-discrete coordination assembly.

Keywords: chirality · helical structures · molecular recognition · N ligands · supramolecular chemistry

One of the paradigmatic branches of supramolecular chemistry is the self-assembly of helicates through the formation of coordinate bonds.[1–3] A large number of various types of ligands with many different metals as coordination centers have been shown to form single-, double-, triple-, or quaternary-stranded, linear-, circular-, or polymeric helices. One challenge in this field is the design of ligands that form helicates of a predictable structure with given metal centers, another is the predetermination of the configuration of these inherently chiral molecular objects,[4–8] and a third is the elucidation of the recognition mechanisms governing the self-assembly processes.

We have shown that ligands of the chiragen family,[9] that is, molecules where two bipyridine units are connected through a chiral bridge, are able to form helicates that are configurationally predetermined. Scheme 1 shows two possible chiragen-type ligands. The 4,5-chiragens form configurationally predetermined dinuclear triple helicates with octahedral coordination centers,[10] whereas the sterically more demanding 5,6-chiragens are suitable for helicate formation with tetrahedral coordination centers, such as Ag^{I}.[11]

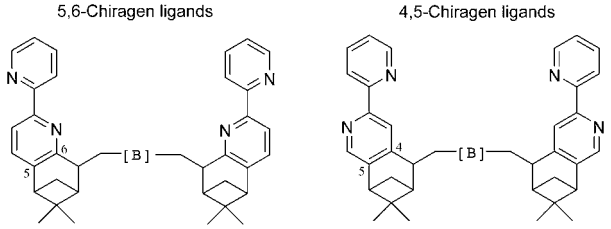

Scheme 1. The chiragen family of ligands.

[a] Dr. O. Mamula, Prof. Dr. A. von Zelewsky, Dr. P. Brodard, Prof. Dr. C.-W. Schläpfer
Department of Chemistry, University of Fribourg
Pérolles, 1700, Fribourg (Switzerland)
Fax: (+41) 26-300-9738
E-mail: alexander.vonzelewsky@unifr.ch

[b] Dr. O. Mamula
Institute of Chemical Sciences and Engineering
Swiss Federal Institute of Technology
1015 Lausanne (Switzerland)

[c] Dr. G. Bernardinelli
Laboratory of X-ray Crystallography, University of Geneva
quai E. Ansermet 24, 1211 Geneva (Switzerland)

[d] Prof. Dr. H. Stoeckli-Evans
Institute of Chemistry, University of Neuchâtel
Bellevaux 51, 2000 Neuchâtel (Switzerland)

Supporting information for this article (crystallographic data and parameters for $[Cu_6(-)\text{-}L1_6](PF_6)_6\cdot(CH_3CN)_3\cdot(C_4H_{10}O)_{1.5}\cdot(H_2O)$, (+)-L1, and (*meso*)-L1 in the CIF format, as well as ES MS spectra for the Cu^{I} complexes with (−)-L1 and L4, respectively) is available on the WWW under http://www.chemeurj.org/ or from the author.

 DOI: 10.1002/chem.200401109

Ligand (−)-L1 (Scheme 2) forms a single-stranded hexanuclear circular helix[11] with Ag^I, whereas the slightly different molecules L2 and L3 (Scheme 2), in which the bridges are derived from dimethylnaphthalenes, lead to polymeric double and monohelices, respectively, in the solid state.[7]

Herein we describe results obtained from an extension of these investigations to a series of Cu^I complexes with the ligands given in Scheme 2: the two enantiomers (−)-L1 and (+)-L1, *m*eso-L1 (the related *meso* form), L4 with an *meta*-xylylene bridge, and L5 and L6 with additional pinene groups annellated to the pyridine rings.

There are two main purposes of the present investigations: 1) The elucidation of the influence on the self-assembly of relatively small variations, either in the ligand structures or in the metals (Cu^I versus Ag^I) and 2) the study of chiral recognition properties by using solutions that do not contain enantiomerically pure ligands.

Results and Discussion

The ligands (−)-L1, (−)-L2, and their Ag^I complexes have been described before.[11,12] (+)-L1 is prepared in the same way as (−)-L1 by starting with (+)-α-pinene. Its X-ray crystal structure (Figure 1a, Table 1) shows that, as expected, the bipyridines are in the *trans* conformation.

The ligand *m*eso-L1 is prepared according to Scheme 3. The low yield of the intermediate monobromo compound 1 is due to the concomitant formation of (−)-L1. In the solid state (Figure 1b, Table 1), besides the common *trans* disposition of the nitrogen atoms in the bipyridines, a *trans* disposition of the bipyridine moieties and pinene groups with respect to the plane of the bridge is observed. The molecule possesses a crystallographic inversion center situated in the aromatic plane of the bridge.

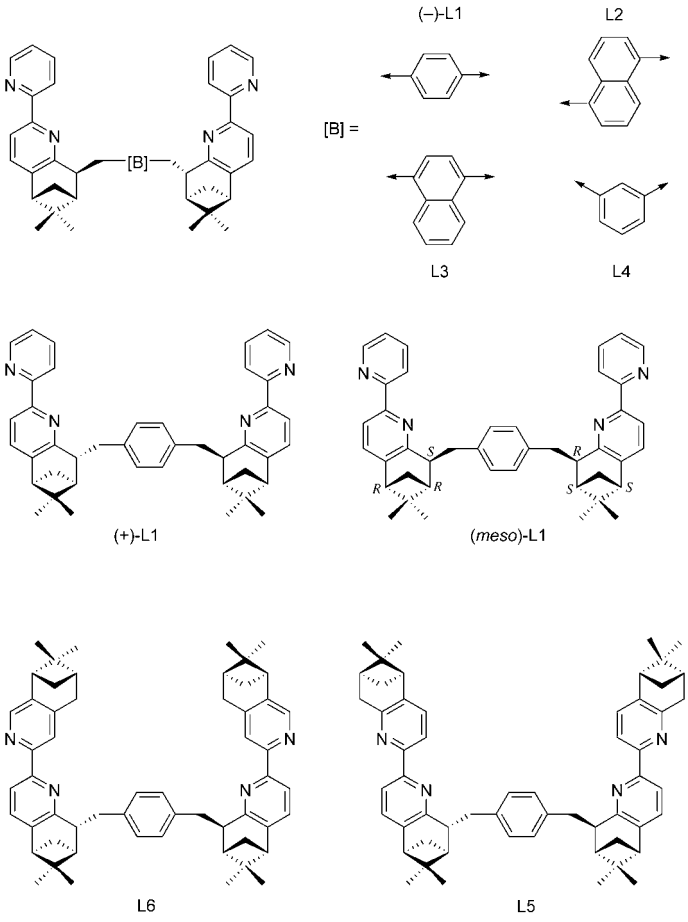

Scheme 2. Different 5,6-chiragen-type ligands that were synthesized for this study.

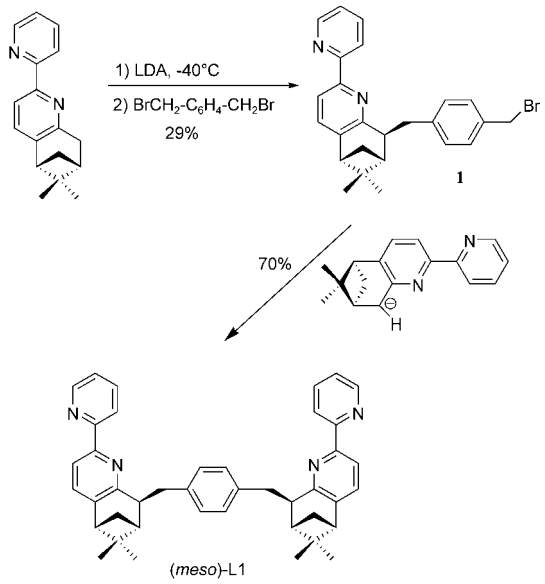

Scheme 3. Synthesis of *meso*-L1 ligand. LDA = lithium diisopropylamide.

Abstract in Romanian: *Două entităţi (−)-5,6-pinen-bipiridină conectate printr-o punte* p-*xiliden constituie ligandul de tip Chiragen (−)-L1. Acesta formează, în reacţie cu o cantitate echimolară de Cu(*I*), un helicat circular hexanuclear enantiopur de chiralitate* P. *Dacă ambii enantiomeri ai ligandului L1 sunt utilizati în această reacţie un amestec de helicati* P *si* M *este obţinut datorita recunoasterii chirale complete: prin complexare ligandul (+) şi cel (−) nu se amestecă. Acest fapt a fost demonstrat prin a) măsurători RMN în care spectre identice cu cele obţinute pentru complecşii cu ligandul chiral pur sunt observate şi b) dicroism circular (DC). Mersul reacţiei se schimbă complet dacă ligandul mezo corespunzător (*meso-*L1) este folosit. În locul helicatului bine definit obţinut înainte, amestecuri oligomerice sunt observate, dovedind astfel rolul deosebit de important pe care chiralitatea ligandului îl poate juca in procesele de auto-asamblare. Variaţii ale structurii ligandului chiral L1 ca de exemplu inlocuirea punţii* p-*xiliden cu una* m-*xiliden (L4) sau introducerea a patru grupe pinen (L5, L6) în loc de două, favorizează asamblajul coordinativ oligomeric.*

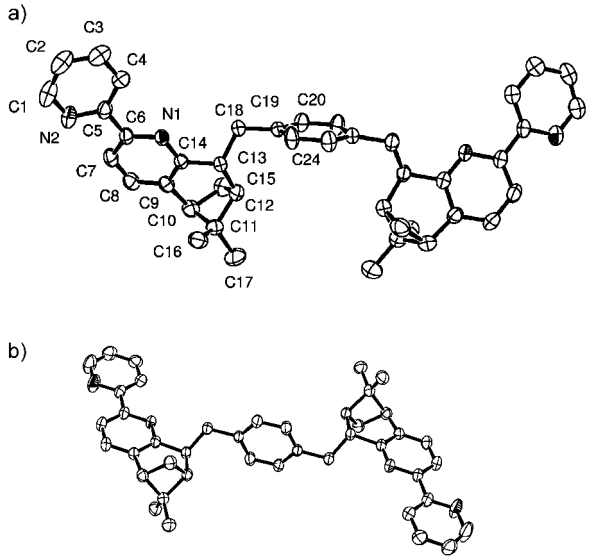

Figure 1. ORTEP view of the ligands a) (+)-L1 and b) *meso*-L1 with 50% probability ellipsoids. The numbering in (b) corresponds to that in (a).

Table 1. X-ray crystallographic data collection and refinement details for (+)-L1 and *meso*-L1.

	(+)-L1	*meso*-L1
Formula	$C_{42}H_{42}N_4$	$C_{42}H_{42}N_4$
M_w	602.88	602.88
crystal appearance	colorless blocks	pale-yellow plates
crystal system	monoclinic	monoclinic
space group	$P2_1$	$P2_1/n$
a [Å]	6.6871(4)	9.4765(6)
b [Å]	17.1382(16)	14.1914(10)
c [Å]	15.4904(10)	12.0662
α [°]	90	90
β [°]	97.392(7)	98.713(9)
γ [°]	90	90
volume [Å^3]	1760(2)	1603.99(19)
Z	2	2
F(000)	644	644
ρ [gcm^{-3}]	1.137	1.248
μ [mm^{-1}]	0.067	0.073
crystal size [mm]	$0.50\times0.40\times0.23$	$0.50\times0.35\times0.20$
T [K]	293(2)	293(2)
radiation [Å]	MoK_α	MoK_α
scan type	ϕ oscillation	ϕ oscillation
θ max [°]	$2.38<\theta<25.93$	$2.23<\theta<25.98$
measured reflections	13869	12436
independent reflections	6488	3118
observed reflections	3643, $I=2\sigma(I)$	1547
refinement parameters	420	219
R	0.0338	0.0394
wR_2	0.0762	0.0877
R (all data)	0.0589	0.0864
wR_2 (all data)	0.0842	0.1000

The synthesis of L5 and L6 was done by starting from L7 and L8[13] and by using the standard procedure for the synthesis of chiragen-type ligands (Scheme 4). It is noteworthy that the deprotonation of L7 takes place at the pinene located in the 5,6-position, probably due to its proximity to the pyridine nitrogen atom.

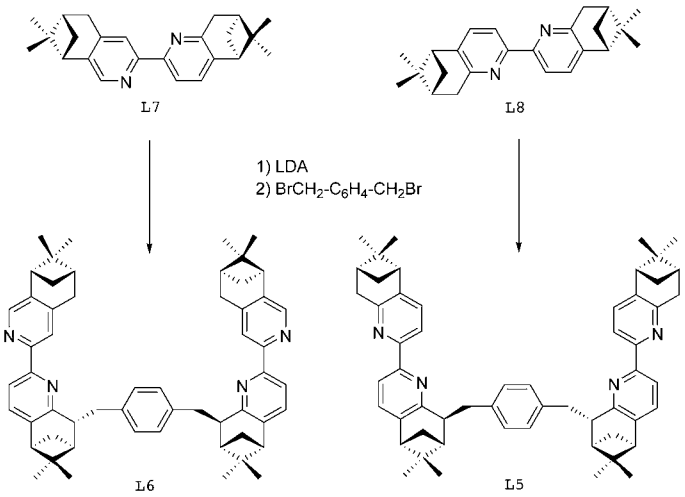

Scheme 4. The final steps in the syntheses of ligands L5 and L6.

Self-assembly with Cu^{I}: An equimolar reaction mixture of $[Cu(CH_3CN)_4]PF_6$ and (−)-L1 yields a product that in several respects is very similar to the species obtained with Ag^{I}.[11] In the solid state, X-ray diffraction studies (Figure 2)

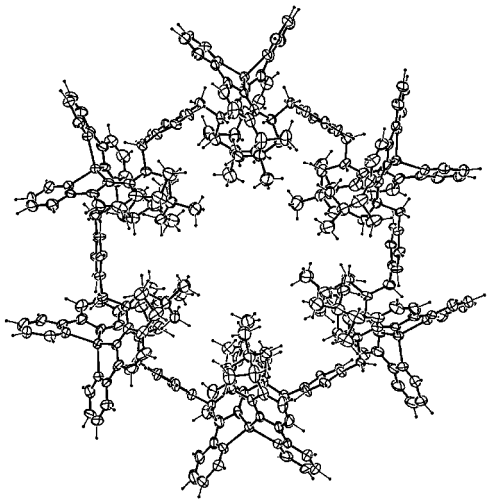

Figure 2. ORTEP view parallel to the C_6 axis of the cation $[Cu_6(-)\text{-}L1_6]^{6+}$ with 30% probability ellipsoids.

show that it is isostructural to the $[Ag_6(-)\text{-}L1_6](PF_6)_6$ circular helix described before. Slight differences occur (see Table 2) due to the larger bite angles observed at the Cu^{I} centers, with the intraannular metal···metal distances of the hexanuclear complex being larger than those observed for the isostructural Ag^{I} compound.

The red color of the copper complexes is due to the well-known metal–ligand charge-transfer (MLCT) band (molar absorption coefficient, $\varepsilon=2000\,M^{-1}cm^{-1}$ for $\lambda_{max}=426$ nm and concentration considered per mol of Cu^+). In solution, similarities between the Cu^{I} and the Ag^{I} complexes again occur. The ^{1}H NMR spectra show that all ligands in the

Table 2. Parameters characterizing the differences between the isostructural compounds $[Ag_6(-)\text{-}L1_6](PF_6)_6$ and $[Cu_6(-)\text{-}L1_6](PF_6)_6$ as determined by X-ray crystallography.

$[M_6(-)\text{-}L1_6](PF_6)_6$	M = Ag^I	M = Cu^I	Δ (Cu^I–Ag^I)
M···M intravicinal [Å]	10.639(2)	10.750(4)	+0.111
M···M intradiagonal [Å]	21.278(2)	21.499(3)	+0.221
M···M around C_3 axis [Å]	8.878(2)	9.162(3)	+0.284
M···M around C_2 axis [Å]	9.961(2)	9.913(3)	−0.048
bite angles [°]	72.0(4), 72.7(5)	81.3(6), 80.8(7)	+8.7[a]
N-M-N chelate plane angles [°]	66.8(2)	85.1(6)	+18.3

[a] Calculated from mean values.

complexes are equivalent and the C_2 symmetry within each ligand is preserved. The signal of the aromatic protons of the bridging xylylene moiety is strongly shifted ($\Delta\delta$ = 1.56 ppm for the Cu^I complex and $\Delta\delta$ = 1.45 ppm for the Ag^I complex; Figure 3). However, whereas the corresponding signal of the Ag^I species is broadened, that of the Cu^I complex is sharp and independent of temperature. It was shown by a detailed investigation (temperature, concentration, pressure dependence, and ^{109}Ag NMR spectroscopy)[14] that an equilibrium between $[Ag_6(-)\text{-}L1_6]^{6+}$ and $[Ag_4(-)\text{-}L1_4]^{4+}$ exists in solution, where the preferred "high-temperature" species is the hexanuclear complex. In the case of the Cu^I system, we deduce from the NMR spectra that one single species is predominant over the whole temperature range from −40 °C up to 38 °C in acetonitrile at the concentrations used for the NMR measurements ($[Cu^+] = 5\times10^{-3}$ M).

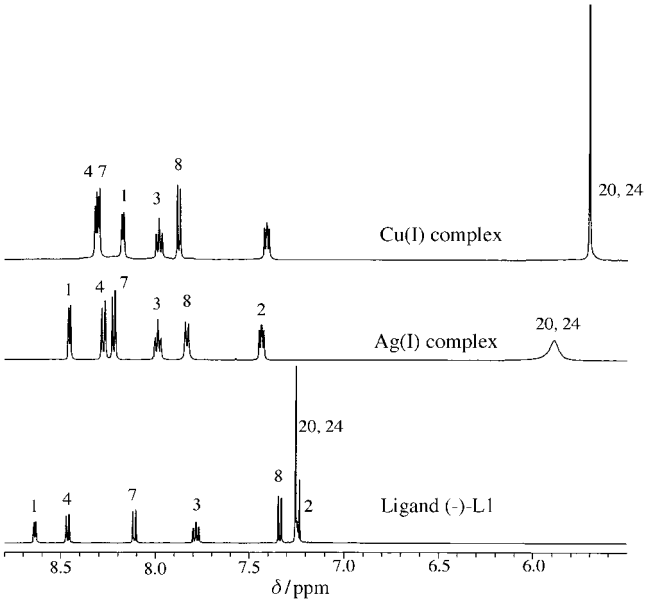

Figure 3. Aromatic region of the ^1H NMR spectra (500 MHz) of the Cu^I and Ag^I complexes with (−)-L1 in CD_3CN and of (−)-L1 in $CDCl_3$ (for solubility reasons; the chemical shifts are identical in CD_3CN).

The MS analysis was first performed by using an API III triple-quadrupole mass spectrometer equipped with an ion-spray source (IS MS). At a Cu^+ concentration of 5×10^{-4} M, the most intense signals (see Figure 4 and Table 3) correspond to a pentanuclear compound $\{[Cu_5(-)\text{-}L1_5](PF_6)_n\}^{5-n}$,

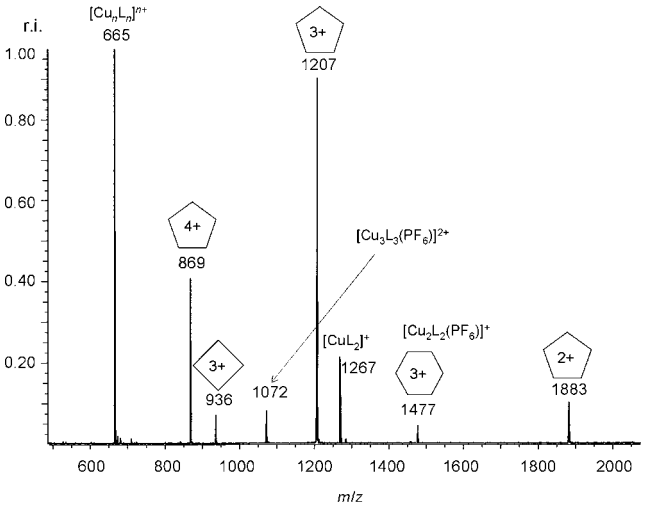

Figure 4. ES MS spectrum of a solution obtained by solubilizing crystals of $[Cu_6(-)\text{-}L1_6](PF_6)_6$ in acetonitrile ($[Cu^+] = 5\times10^{-4}$ M).

Table 3. Principal peaks in the ES MS spectrum of $[Cu_6(-)\text{-}L1_6](PF_6)_6$ and their attributions.

m/z	Cu^I complex species with (−)-L1
665.2	$[CuL1]^+$, $[Cu_2L1_2]^{2+}$
869.0	$\{[Cu_5L1_5]PF_6\}^{4+}$
936.6	$\{[Cu_4L1_4]PF_6\}^{3+}$
1071.8	$\{[Cu_3L1_3]PF_6\}^{2+}$
1207.0	$\{[Cu_5L1_5](PF_6)_2\}^{3+}$
1267.5	$[CuL1_2]^+$
1477.4	$\{[Cu_6L1_6](PF_6)_3\}^{3+}$ and $\{[Cu_2L1_2]PF_6\}^+$
1883.0	$\{[Cu_5L1_5](PF_6)_3\}^{2+}$

but signals of lower intensities assigned to hexa-, tetra-, tri-, di-, and mononuclear complexes are also present. At lower concentrations (5×10^{-5} M, 5×10^{-6} M), the intensities of the peaks corresponding to the pentanuclear multicharged complexes decrease and peaks attributed to decomposition products such as $[Cu(-)\text{-}L1_2]^+$ become more intense. It is known that, in general, ES MS reflects qualitatively the species present in solution and that the most abundant species observed in the conditions of the experiment (gas phase) can be different from the complex formed by crystallization. Moreover, the resolution of a quadrupole mass analyzer is not sufficient to resolve multicharged ions. This makes the assignment of certain multicharged peaks difficult. For example, the peak at m/z 1070 can correspond to $\{[Cu_6(-)\text{-}L1_6](PF_6)_2\}^{4+}$ or $\{[Cu_3(-)\text{-}L1_3](PF_6)\}^{2+}$. The signal at m/z 1477.9 can be attributed to $\{[Cu_6(-)\text{-}L1_6](PF_6)_3\}^{3+}$, $\{[Cu_4(-)\text{-}L1_4](PF_6)_2\}^{2+}$, or $\{[Cu_2(-)\text{-}L1_2](PF_6)\}^+$. To clarify this aspect, another series of measurements was performed with a

Bruker FTMS 4.7 T BioApex II by using a standard electrospray source. Unambiguous assignments have been achieved in this way (Figure 4, Table 3; see the Supporting Information for expansions of the most important peaks).

It is noteworthy to add here that the dinuclear and trinuclear complexes observed by MS must have a linear structure because of the length and rigidity of the bridge. However, the tetra- and pentanuclear complexes can adopt circular structures (Figure 5), which would probably represent a gain

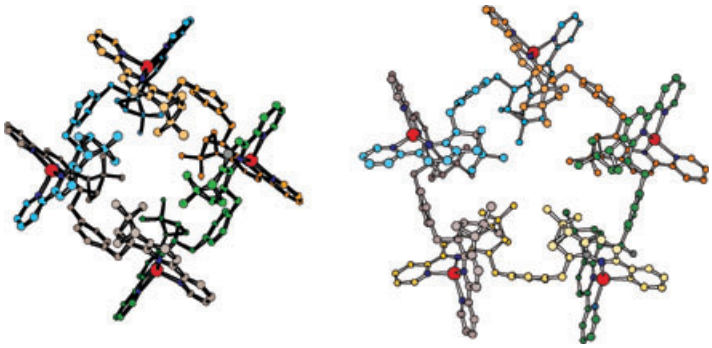

Figure 5. Molecular models of $[Cu_4(-)\text{-}L1_4](PF_6)_4$ (left) and $[Cu_5(-)\text{-}L1_5](PF_6)_5$ (right) obtained by using Hyperchem software with the bonding parameters observed by X-ray crystallography for $[Cu_6(-)\text{-}L1_6](PF_6)_6$.

in energy relative to linear structures in which one bipyridine arm of one ligand is free and one tetrahedral Cu^I metal center coordinates to only one bipyridine unit of the tetradentate ligand. All coordination sites are thus saturated in the cyclic form, but not in the linear form.

Chiral recognition: Chiral recognition at the level of intermolecular interactions is a phenomenon that has been studied very thoroughly in many heterogeneous systems, that is, in complexes of the type $[M(bpy)_3](PF_6)_2$ where $M = Ru^{II}$, Zn^{II}, Ni^{II} (bpy = 2,2′-bipyriyl).[15–17] If a crystalline phase is formed from molecules or ions in solution, various types of chiral recognition can occur.[18] When a crystal is formed from a racemate in solution, the most frequent occurrence is the formation of an ordered racemic crystal, that is, each unit cell contains an equal number of the two enantiomers of the racemate. Another less frequently encountered possibility is the formation of a racemic conglomerate by spontaneous resolution of the racemate or, in more rare cases, the formation of a solid solution where the two enantiomers are distributed randomly in the crystal. This latter case shows that chiral recognition does not always take place upon crystallization.[19]

Crystals are self-assembled architectures, which are "infinite" on the molecular scale. Self-assembly reactions that yield finite molecular species follow the same principles if the building blocks of the supramolecular architectures are chiral species. A particularly interesting problem is the chiral recognition between so-called "mixtures of instructed ligands".[20] This phenomenon is referred to as chiral self-recognition (or homorecognition, when the same enantiomer from a racemic mixture of ligands is present in the final homochiral architecture) and as chiral self-discrimination (or heterorecognition, when both enantiomers of the racemic mixture are present in the final heterochiral compound).

However, in the field of coordination supramolecular chemistry, only a few examples have been shown to possess these intriguing properties. Under complexation with Cu^I cations, racemic mixtures of chiral ligands form mono-[21,22] or dinuclear[23,24] species with homorecognition related to the "narcissistic" self-sorting phenomena in (supra)molecular systems.[25,26] Homochiral formation of a) a trinuclear capsule containing Ag^I and chiral tris(oxazoline)-type ligands[27] and b) a tetrahedral cluster with Ga^{III} and chiral bis-catecholamide ligands[28] have been also reported.

Heterochiral self-assembly processes lead to the formation of Pd^{II}-containing cages with aromatic macrocyclic ligands.[29] Synthesis of mononuclear Pt^{II} complexes containing ligands of opposite chirality selected from an atropoisomeric racemic mixture have been also reported.[30] Tridentate C_2-symmetric bis(oxazolinyl)pyridine ligands have shown various heterorecognition capabilities in octahedral Co^{II} complexes as well; this has been explained in terms of interligand repulsion between substituents.[31] As a consequence, the Cu^{II} complexes with the same type of ligand show nonlinear effects when used as enantioselective catalysts.[32]

A special example of partial homochiral recognition between racemic anions (of the trisphate type) and racemic Ru^{II} complexes has been published by Lacour and co-workers.[33]

The facile availability of both enantiomers of ligand L1 prompted us to investigate the reaction with Cu^I in a solution containing an artificial racemic mixture of the two enantiomeric forms of ligand L1 and a Cu^I:$L1_{total}$ ratio of 1:1. Examination by CD spectroscopy revealed that the CD spectrum is completely void of any signals. This is just a confirmation that the solution does, indeed, contain a racemic mixture of the two ligands. The ^1H NMR spectra, on the contrary, are in every respect identical to those obtained from solutions containing the complex obtained from the enantiopure ligand. The conclusion is that a *racemate of ligands* yields *a racemate of the chiral self-assembled structures* (Figure 6). No mixing of the two enantiomers occurs within the supramolecular architecture formed in the self-assembly reaction. This behavior is analogous to the spontaneous resolution of the two enantiomers into enantiomorphic crystals.

A supplementary confirmation for the chiral recognition came from the CD spectra of Cu^I complexes obtained with nonracemic mixtures of (−)-L1 and (+)-L1. As an example, we measured the $\Delta\varepsilon$ values in solutions containing (−)-L1 and (+)-L1 in molar ratio of a) 3:1 or b) 2:1 and a Cu^I:$L1_{total}$ molar ratio of 1:1 ($[Cu^+] = 1.5 \times 10^{-4}$ M, $\lambda = 316$, 269 nm). In case a, the $\Delta\varepsilon$ value is 50% of that for a corresponding solution containing only the enantiopure (−)-L1 ligand, a result meaning that the composition of this solution is 75%

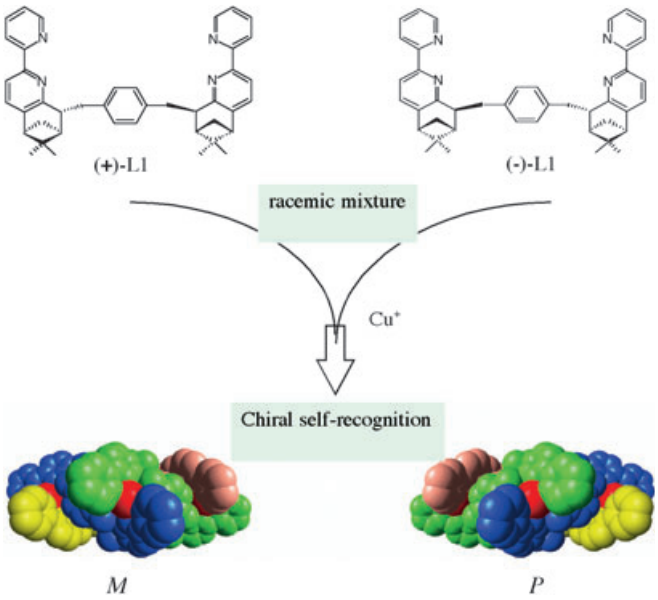

Figure 6. Complete self-recognition between the enantiomers of L1, with the formation of left-handed circular helicate *M*-$[Cu_6(+)\text{-}L1_6](PF_6)_6$ and right-handed circular helicate *P*-$[Cu_6(-)\text{-}L1_6](PF_6)_6$. The representation of the view perpendicular to the C_6 axis of $[Cu_6(-)\text{-}L1_6]^{6+}$ was obtained from X-ray diffraction data, whereas the view of $[Cu_6(+)\text{-}L1_6]^{6+}$ is the mirror image of the former.

right-handed helix and 25% left-handed helix. Therefore, the resulting CD signals will represent only 50% excess of CD activity; this corresponds to a 50% *ee* value for the enantiomeric complex. This is confirmed by case b as well, where the value of the CD signal represents 25% *ee*. Attempts to obtain crystals of the solutions containing a mixture of L1 resulted always in solids yielding low-quality diffraction patterns. Unit-cell measurements of these crystals show identical values to those of the enantiopure material, a fact indicating conglomerate crystallization.

An attempt was also made to study chiral recognition in analogous Ag^I complexes. Yet, all solutions containing Ag^+ ions and both enantiomers of L1 showed strong line broadening of the signals in the ^{1}H NMR spectra, concomitantly with the development of an amorphous precipitate.

Since the chiral ligands have been shown to yield selectively self-recognizing species with Cu^I, we investigated also the corresponding *meso*-L1 ligand, which is composed of one (*S*,*S*)- and one (*R*,*R*)-pinene–bipyridine moiety. This overall achiral ligand (the two chiral centers in the bridge also have opposite configurations) behaves completely differently towards complexation. Addition of this ligand to solutions of Cu^+ or Ag^+ in acetonitrile/chloroform yields precipitates that could not be solubilized (even by heating) in various solvents, a fact indicating the formation of coordination polymers. Thus, the chiral ligand seems to control the stereoselective formation of relatively small supramolecular assemblies, whereas the *meso* ligand leads to randomly assembled polymeric species. Enhancement of stereoselectivity in self-assembly processes by the introduction of chiral ligands seems to be a general phenomenon.[34]

The *meta*-xylylene-bridged ligand[14] L4 (Scheme 2) was also investigated. At room temperature, broad signals are observed in the ^{1}H NMR spectrum. At lower temperatures, a narrow line spectrum is observed (Figure 7) in which, as in the case of ligand L1, all the ligands are equivalent and the

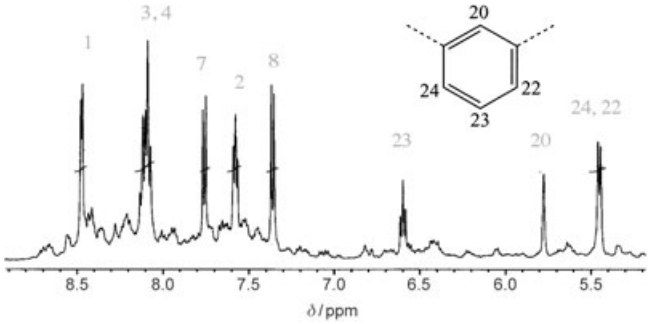

Figure 7. Aromatic region of the ^{1}H NMR (500 MHz) spectrum of $[Cu_nL4_n](PF_6)_n$ at −40 °C in CD_3CN.

C_2 symmetry through each of them is preserved. All protons in the bridging group are strongly shifted with respect to the free ligand. The three different proton signals from the bridge experience quite different shifts ($\Delta\delta$(H20) = 1.48, $\Delta\delta$(H23) = 0.61, $\Delta\delta$(H24/22) = 1.72 ppm). The conclusion from these observations is that the *meta*-xylylene-bridged ligand L4 forms a circular helicate in solution, since only a circular structure of a polynuclear species is compatible with the high symmetry indicated by the ^{1}H NMR spectra at low temperatures. The CD spectrum shows an exciton coupling of the same sign as in $[Cu_6(-)\text{-}L1_6]^{6+}$; this indicates that the same absolute local configuration of the metal centers is Λ.

The ES MS shows a strong predominance of two signals belonging to one complex species, namely, $[Cu_3L4_3]^{3+}$ (100%) and $\{[Cu_3L4_3]PF_6\}^{2+}$ (80%), but signals with an intensity lower than 10% have been attributed to penta-, tetra-, di-, and mononuclear species (see the Supporting Information).

The two ligands having pineno groups annelated to both rings in one bipyridine moiety, L5 and L6 (Scheme 2), were also investigated with respect to their complex formation with Cu^I. The ^{1}H NMR spectra show a multitude of broad signals at room temperature that did not sharpen considerably upon cooling to −40 °C. From a 1:1 molar ratio of L6 and Cu^+ in acetonitrile, a microcrystalline precipitate is formed slowly. It is assumed that several different, perhaps polymeric, associates are formed.

Conclusion

Chiral recognition is a general and essential phenomenon in chemical biology.[35,36] We have shown before that certain chiral bipyridine-type ligands form well-defined species through coordinative self-assembly processes. In this publication it is proven that these processes can occur in a highly

controlled manner with respect to chiral self-recognition. Moreover, as in the natural systems, chirality seems to be essential for the reaction pathway. A ligand that yields a circular helicate as a chiral isomer produces polymeric species when the *meso* form is used. Further studies with ligands from the same family, but with more important structural variations (different bridges or binding-site environments), again show a loss of preference for the formation of well-defined, discrete species. Thus, the design of new self-assembling systems is still a complicated task, which can only be successfully accomplished through a mixture of knowledge, intuition, conjecture, and serendipity.

Experimental Section

The starting materials and solvents were of the best available commercial grade and were used without further purification, except THF, which was distilled from a mixture of Na/benzophenone. The NMR spectra were recorded on a Varian Gemini 300 or Bruker Avance DRX500 spectrophotometer by using the residual nondeuterated solvent peak as an internal reference. Mass spectra were measured on a Hewlett–Packard 5988 A quadrupole mass spectrometer with an electron-ionization source or on a Bruker FTMS 4.7 T Bioapex II spectrometer with a standard electrospray ion source. UV/Vis spectroscopic measurements were recorded by using a Perkin–Elmer Lambda 40 spectrophotometer. Wavelengths are given in nm and molar absorption coefficients in $M^{-1}cm^{-1}$. Circular dichroism spectra were recorded on a Jasco J-715 spectropolarimeter and the results are given in $\Delta\varepsilon$ ($M^{-1}cm^{-1}$).

1: Dried THF (20 mL) was placed in a three-necked flask, under argon, and cooled down. When the temperature was stabilized at −20 °C, diisopropylamine (5.37 mmol, 0.76 mL) and *n*-butyllithium (5 mmol, 3.06 mL, 1.6 M in hexane) were added successively. The temperature was increased to 0 °C (ice bath) for 10 min and then the mixture was cooled to −40 °C (isopropyl alcohol bath). (+)-5,6-pinene bipyridine (1 g, 4 mmol) dissolved in THF (10 mL) was added over a period of 40 min and the resulting dark-blue solution was stirred at −40 °C for 2 h. This solution was carefully transferred (20 min) through a canula into a Schlenk flask containing α,α′-dibromo-*p*-xylene (3.8 mmol, 1 g) dissolved in THF (150 mL) and kept at −45 °C. The colorless solution obtained was stirred at room temperature for 1 h. After solvent removal, the white solid that resulted was purified by column chromatography (SiO_2, hexane/EtOAc 7:1). Yield: 29 %; ^{1}H NMR (300 MHz, $CDCl_3$, 25 °C): δ = 8.59 (br, 2H), 8.39 (d, 1H), 8.29 (d, 1H), 8.09 (d, 1H), 8.00 (d, 1H), 7.71 (br d, 2H), 7.25 (m, 2H), 4.44 (s, 2H), 3.72 (d, 1H,), 3.33 (d, 1H), 2.72–2.62 (m, 2H), 2.5 (d, 1H), 2.31 (br, 1H), 1.33 (s, 3H), 1.23 (d, 1H), 0.55 ppm (s, 3H); MS (FAB, *m*-nitrobenzyl alcohol): *m*/*z* (%): 433 (15) $[L]^+$, 249 (50) $[L-C_{17}H_{17}N_2]^+$.

***meso*-L1**: By using as starting compounds the ligand (−)-5,6 pinene bipyridine (125.2 mg, 0.5 mmol) and the monobromocompound **1** (0.5 mmol, 216.5 mg), the synthesis was carried out according to the standard procedure used for chiragen-type ligands.[11] The purification was achieved by column chromatography (SiO_2, hexane/EtOAc/triethylamine (TEA) 4:1:0.1, R_f = 0.16) and recrystallization from $CH_3OH/CHCl_3$. Yield: 70 %; ^{1}H NMR (300 MHz, $CDCl_3$, 25 °C): δ = 8.65 (ddd, 2H, $^3J_{1,2}$ = 4.8, $^4J_{1,3}$ = 1.8, $^5J_{1,4}$ = 0.9 Hz; H(1)), 8.47 (d, 2H, $^3J_{4,3}$ = 8.0 Hz; H(4)), 8.13 (d, 2H, $^3J_{7,8}$ = 7.8 Hz; H(7)), 7.80 (ddd, 2H, $^3J_{3,4}$ = 7.9, $^3J_{3,2}$ = 7.6, $^4J_{3,1}$ = 1.7 Hz; H(3)), 7.34 (d, 2H, $^3J_{8,7}$ = 7.8 Hz; H(8)), 7.26 (s, 4H, H(20,24)), 7.25 (m, 2H, H(2)), 3.82 (dd, 2H, $^2J_{18b,18a}$ = 13.7, $^3J_{18b,13}$ = 3.8 Hz; H(18b)), 3.38 (ddd, 2H, $^3J_{13,18b}$ = 3.5, $^3J_{13,18a}$ = 10.8, $^3J_{13,12}$ = 2.7 Hz; H(13)), 2.81 (dd, 2H, $^3J_{10,15b}$ = 5.6, $^4J_{10,12}$ = 5.6 Hz; H(10)), 2.72 (dd, 2H, $^2J_{18a,18b}$ = 13.7, $^3J_{18a,13}$ = 10.8 Hz; H(18a)), 2.58 (ddd, 2H, $^3J_{15b,10}$ = 5.6, $^3J_{15b,12}$ = 5.6, $^2J_{15b,15a}$ = 9.8 Hz; H(15b)), 2.16 (ddd, 2H, $^3J_{12,15b}$ = 5.6, $^4J_{12,10}$ = 5.6, $^3J_{12,13}$ = 3 Hz; H(12)), 1.43 (d, 2H, $^2J_{15a,15b}$ = 9.9 Hz; H(15a)), 1.36 (s, 6H, H(17)), 0.62 ppm (s, 6H, H(16)); ^{13}C NMR (75.44 MHz, $CDCl_3$, 25 °C): δ = 158.9 (q), 156.7 (q), 153.4 (q), 148.8 (C(1)), 142.5 (q), 138.6 (q), 137.0 (C(3)), 133.8 (C(8)), 129.3 (C(20), C(21), C(23), C(24)), 123.2 (C(2)), 121.0 (C(4)), 118.1 (C(7)), 47.0 (C(10)), 46.3 (C(13)), 42.8 (C(12)), 41.2 (q, C(11)), 38.5 (C(18)), 28.4 (C(15)), 26.4 (C(17)), 20.9 ppm (C(16)); MS (FAB, *m*-nitrobenzyl alcohol): *m*/*z* (%): 603 (40) $[M]^+$, 249.2 (35) $[M-C_{17}H_{17}N_2]^+$, 207.2; UV/Vis (1.08 mg in 15 mL CH_2Cl_2)): λ (ε) = 255 (4×10^4), 294 (6.9×10^4), 308 nm (4.7×10^4 $M^{-1}cm^{-1}$, sh); elemental analysis: calcd (%) for $C_{42}H_{42}N_4\cdot1.5H_2O$: C 80.09, H 7.20, N 8.90; found: C 79.98, H 7.32, N 8.84.

L5: By using as starting compounds L8 and α,α′-dibromo-*p*-xylene, the synthesis was carried out according to the standard procedure used for chiragen-type ligands.[11] The crude product was purified by column chromatography (SiO_2, hexane/diethyl ether/TEA 5:1:0.1, R_f = 0.22). Yield: 40 %; ^{1}H NMR ($CDCl_3$, 300 MHz): δ = 8.10 (d, 2H, $^3J_{7,8}$ = 7.75 Hz; H(7)), 8.05 (d, 2H, $^3J_{4,3}$ = 7.7 Hz; H(4)), 7.31 (d, 4H, H(8), H(3)), 7.25 (s, 4H, H(20), H(24), 3.84 (dd, 2H, $^2J_{18b,18a}$ = 13.6, $^3J_{18b,13}$ = 3.7 Hz; H(18b)), 3.39 (d, 2H, $^3J_{13,18a}$ = 8.1 Hz; H(13)), 3.17 (d, 4H, $^3J_{13',12'}$ = 2.53 Hz; H(13′)), 2.81–2.52 (10H, H(15b), H(15b′), H(18a), H(10), H(10′), superposed), 2.38 (ddt, 2H, $^3J_{12',15'}$ = 5.3, $^4J_{12',10'}$ = 5.3, $^3J_{12',13'}$ = 2.5 Hz; H(12′)), 2.14 (ddt, 2H, $^3J_{12,15}$ = 5.6, $^4J_{12,10}$ = 5.6, $^3J_{12,13}$ = 3.1 Hz; H(12)), 1.44 (d, 2H, $^2J_{15a,15b}$ = 9.7 Hz; H(15a)), 1.40 (s, 6H, H(17′)), 1.40 (s, 6H, H(17)), 1.30 (d, 2H, $^2J_{15a',15b'}$ = 9.8 Hz; H(15a′)), 0.65 (s, 6H, H(16′)), 0.61 ppm (s, 6H, H(16)); ^{13}C NMR (75.44 MHz, $CDCl_3$, 25 °C): δ = 158.7 (q), 156.3 (q), 154.4 (q), 154.0 (q), 141.6 (q), 138.6 (q), 133.8 and 133.7 (C(8) and C(3)), 129.3 (C-(20, 24)), 117.8 and 117.7 (C(7) and C(4)), 46.9 (C(10′)), 46.5 (C(10)), 46.2 (C(13)), 42.8 (C(12)), 41.3 (q, C(11)), 40.4 (C(12′)), 39.5 (q), 38.5 (C(18)), 36.8 (C(13′)), 32.0 (C(15′)), 28.4 (C(15)), 26.4(C(17)), 26.1-(C(17′)), 21.3 (C(16′)), 20.9 ppm (C(16)); MS (FAB, *m*-nitrobenzyl alcohol): *m*/*z* (%): 791 $[M]^+$ (100), 343 $[C_{24}H_{26}N_2]^+$ (50); UV/Vis (CH_2Cl_2, $c = 1.3\times10^{-4}$ M, 0.1 cm): λ (ε) = 257 (2.5×10^4, sh), 263 (2.7×10^4), 302 (5×10^4), 313 nm (3.8×10^4 $M^{-1}cm^{-1}$, sh); elemental analysis: calcd (%) for $C_{56}H_{62}N_4\cdot0.5H_2O$: C 84.06, H 7.94, N 7.0; found: C 84.20, H 8.19, N 6.83.

L6: By using as starting compounds L7 and α,α′-dibromo-*p*-xylene, the synthesis was carried out according to the standard procedure used for chiragen-type ligands.[11] The purification was achieved by recrystallization from warm ethanol. Yield: 47 %; R_f = 0.19 (hexane/EtOAc/TEA 4:1:0.1); ^{1}H NMR ($CDCl_3$, 300 MHz): δ = 8.38–8.30 (6H, H(7), H(4), H(1), superposed), 7.43 (d, 2H, $^3J_{8,7}$ = 7.9 Hz; H(8)), 7.29 (s, 4H, H(20), H(24)), 3.87 (dd, 2H, $^2J_{18b,18a}$ = 13.7, $^3J_{18b,13}$ = 3.75 Hz; H(18b)), 3.45 (ddd, 2H, $^3J_{13,18b}$ = 3.75, $^3J_{13,12}$ = 6.0 Hz; H(13)), 3.17 (d, 4H, $^3J_{13',12'}$ = 4.9 Hz; H-(13′)), 2.94 (dd, 2H, $^3J_{10',15b'}$ = 5.3, $^3J_{10',12'}$ = 5.3 Hz; H(10′)), 2.84 (dd, 2H, $^3J_{10,15b}$ = 5.6, $^3J_{10,12}$ = 5.6 Hz; H(10)), 2.75 (4H, H(15b′), H(18a), superposed), 2.59 (ddd, 2H, $^2J_{15b,15a}$ = 10.2, $^3J_{15b,10}$ = 5.6, $^3J_{15b,12}$ = 5.6 Hz; H(15b)), 2.37 (ddt, 2H, $^3J_{12',15b'}$ = 5.6, $^3J_{12',10'}$ = 5.6, $^4J_{12',13'}$ = 2.9 Hz; H(12′)), 2.15 (ddt, 2H, $^3J_{12,15b}$ = 6.0, $^4J_{12,10}$ = 5.6, $^3J_{12,13}$ = 2.7 Hz; H(12)), 1.44 (d, 2H, $^2J_{15a,15b}$ = 10.2 Hz; H(15a)), 1.45 (s, 6H, H(17′)), 1.37 (s, 6H, H(17)), 1.24 (d, 2H, $^2J_{15a',15b'}$ = 9.9 Hz; H(15a′)), 0.68 (s, 6H, H(16′)), 0.63 ppm (s, 6H, H(16)); ^{13}C NMR (75.44 MHz, $CDCl_3$, 25 °C): δ = 159.3 (q), 143.6 (q), 138.3 (C(8)), 134.0 (C(7)), 129.1 (C(20, 24)), 121.4 and 118.9 (C(4) and C(1)), 46.9 (C(10)), 46.0 (C(13)), 44.4 (C(10′)), 42.4 (q), 41.1 (C(12)), 39.7 (q), 39.1 (C(12′)), 38.3 (C(18)), 33.5 (C(13′)), 31.5 (C(15′)), 28.1 (C(15)), 26.2-(C(17)), 25.6 (C(17′)), 21.3 (C(16′)), 20.8 ppm (C(16)); MS (FAB, *m*-nitrobenzyl alcohol): *m*/*z* (%): 791$[M]^+$ (100), 343 $[C_{24}H_{26}N_2]^+$ (50); CD (CH_2Cl_2, $c = 1.6\times10^{-4}$ M, 0.1 cm): λ ($\Delta\varepsilon$) = 257 (−2), 301 nm (−8 $M^{-1}cm^{-1}$); UV/Vis (CH_2Cl_2, $c = 1.6\times10^{-4}$ M, 0.1 cm): λ (ε) = 257 (2.6×10^4, sh), 262 (2.8×10^4), 299 (4.6×10^4), 310 nm (3.5×10^4 $M^{-1}cm^{-1}$, sh); elemental analysis: calcd (%) for $C_{56}H_{62}N_4\cdot1.5H_2O$: C 82.21, H 8.01, N 6.85; found: C 82.3, H 8.01, N 6.67.

$[Cu_6(-)\text{-}L1_6](PF_6)_6$: A solution of (−)-L1·$H_2O$ (0.1 mmol, 62.1 mg) in acetonitrile/chloroform (1:1) was added under argon to a solution $[Cu(CH_3CN)]PF_6$ (0.1 mmol, 37.3 mg) in acetonitrile prepared according to the literature procedure.[37] The mixture immediately became red. The solvent was entirely evaporated under reduced pressure and the residue was taken up in a minimum amount of acetonitrile and precipitated with diethyl ether. Yield: 96 %; R_f = 0.47 (acetonitrile/butanol/water/KNO_3 (sat.) 4:1:1:0.1); suitable crystals for X-ray crystal analysis were obtained by slow diffusion of diethyl ether into an acetonitrile solution of the Cu^I complex; ^{1}H NMR (CD_3CN, 500 MHz, 25 °C): δ = 8.31 (d, 2H, $^3J_{4,3}$ =

8.2 Hz; H(4)), 8.30 (d, 2H, $^3J_{7,8}$=8.0 Hz; H(7)), 8.17 (d, 2H, $^3J_{1,2}$=4.6 Hz; H(1)), 7.98 (ddd, $^3J_{3,4}$=8.2, $^3J_{3,2}$=7.8, $^4J_{3,1}$=1.6 Hz; H(3)), 7.87 (d, 2H, $^3J_{8,7}$=8.0 Hz; H(8)), 7.40 (ddd, 2H, $^3J_{2,3}$=7.8, $^3J_{2,1}$=4.6, $^3J_{2,4}$=0.9 Hz; H(2)), 5.70 (s, 4H, H(20, 24)), 3.68 (dd, 2H, $^2J_{18b,18a}$=13.0, $^3J_{18b,13}$= 3.3 Hz; H(18b)), 3.02 (dd, 2H, $^4J_{10,12}$=5.7, $^3J_{10,15b}$=5.7 Hz; H(10)), 2.69 (d, 2H, $^3J_{13,18a}$=11.7 Hz; H(13)), 2.54 (ddd, $^2J_{15b,15a}$=10.1, $^3J_{15b,12}$=5.7, $^3J_{15b,10}$=5.7 Hz; H(15b)), 2.27 (dd, 2H, $^2J_{18a,18b}$=13.0 Hz; H(18a)), 1.59 (d, 2H, $^2J_{15a,15b}$=10.1 Hz; H(15a)), 1.33 (ddd, 2H, $^3J_{12,15b}$=5.7, $^3J_{12,13}$=2.8, $^4J_{12,10}$=5.7 Hz; H(12)), 1.12 (s, 6H, H(17)), 0.02 ppm (s, 6H, H(16)); ^{13}C NMR (CD_3CN, 125.75 MHz, 25 °C): δ=159.57 (q), 153.26 (q), 152.02 (q), 148.99 (C(1)), 146.79 (q), 139.56 (C(3)), 137.62 (q), 136.66 (C(8)), 129.27 (C(20), C(21), C(23), C(24)), 127.16 (C(2)), 122.65 (C(4)), 121.89 (C(7)), 49.7 (C(13)), 47.33 (C(10)), 43.14 (C(12)), 41.23 (q, C(11)), 36.7 (C(18)), 27.94 (C(15)), 26.45 (C(17)), 22.41 ppm (C(16)); CD (CH_3CN, $c=1.2\times10^{-5}$ M [CuL1]$^+$): λ ($\Delta\varepsilon$)=316 (14), 269 nm (-4 M^{-1}cm^{-1}); UV/Vis (CH_3CN, $c=3.7\times10^{-5}$ M [CuL1]$^+$): λ (ε)=230 (2.93×10^4, sh), 254 (2.51×10^4), 294 (3.5×10^4), 426 (2×10^3), 520 nm (517 M^{-1}cm^{-1}, sh); ES MS ($c=5\times10^{-4}$ M [CuL1]$^+$) (%): 665.27 $[Cu_nL1_n]^{n+}$ (100), 869.08 $\{[Cu_5L1_5]PF_6\}^{4+}$ (40), 936.68 $\{[Cu_4L1_4]PF_6\}^{3+}$ (8), 1071.88 $\{[Cu_3L1_3]PF_6\}^{2+}$ (9), 1207.08 $\{[Cu_5L1_5](PF_6)_2\}^{3+}$ (90), 1267.59 $[CuL1_2]^+$ (20), 1477.48 $\{[Cu_6L1_6](PF_6)_3\}^{3+}$ and $\{[Cu_2L1_2]PF_6\}^+$ (5), 1883.07 $\{[Cu_5L1_5](PF_6)_3\}^{2+}$ (10); other fragmentations observed had intensities lower than 1%: $\{[Cu_6L1_6]PF_6\}^{5+}$, $\{[Cu_6L1_6](PF_6)_2\}^{4+}$, $\{[Cu_3L1_3]PF_6\}^{2+}$, $\{[Cu_6L1_6](PF_6)_4\}^{2+}$, $\{[Cu_3L1_3](PF_6)_2\}^+$; elemental analysis: calcd (%) for $Cu_6C_{252}H_{252}N_{24}P_6F_{36}$: C 62.18, H 5.22, N 6.91; found: C 61.95, H 5.40, N 6.77.

$[Cu_nL4_n](PF_6)_n$: A similar procedure to that used for the synthesis of $[Cu_6(-)\text{-}L1_6](PF_6)_6$ was used. The yield was higher than 95%. ^{1}H NMR (CD_3CN, 300 MHz, -40 °C): δ=8.5 (d, 2H, $^3J_{1,2}$=4.7 Hz; H(1)), 8.1 (m, 4H; H(3), H(4)), 7.75 (d, 2H, $^3J_{7,8}$=8.0 Hz; H(7)), 7.55 (dd, 2H, $^3J_{2,3}$= 6.0, $^3J_{2,1}$=5.3 Hz; H(2)), 7.35 (d, 2H, $^3J_{8,7}$=8.0 Hz; H(8)), 6.62 (dd, 1H, $^3J_{23,22}$=7.6, $^3J_{23,24}$=7.6 Hz; H(23)), 5.78 (s, 1H; H(20)), 5.45 (d, 2H, $^3J_{22(24),23}$=7.6 Hz; H(24), H(22)), 3.95 (2H), 2.8 (m, 4H), 2.3 (2H), 2.2 (2H), 1.7 (2H), 1.2 (m, 8H), 0.5 ppm (6H); ES MS ($c=2\times10^{-4}$ M [CuL4]$^+$) (%): 665.9 $[Cu_3L4_3]^{3+}$ (100), 1071 $\{[Cu_3L4_3]PF_6\}^{2+}$ (25); other fragmentations observed had intensities lower than 10%: 936 $\{[Cu_4L4_4]PF_6\}^{3+}$; 1207 $\{[Cu_5L4_5](PF_6)_2\}^{3+}$; 1269 $[CuL4_2]^+$, 1476 $\{[Cu_2L4_2]PF_6\}^+$; UV/Vis (CH_3CN, $c=2.1\times10^{-4}$ M [CuL]$^+$, 0.1 cm): λ (ε)= 260 (2.3×10^4, sh), 273 (2.7×10^4), 299 (2.7×10^4, sh), 306 (2.9×10^4), 419 nm (0.2×10^4 M^{-1}cm^{-1}); CD (CH_3CN, $c=2.1\times10^{-4}$ M, 0.1 cm): λ ($\Delta\varepsilon$)=234 (+9), 264 (−8), 317 nm (+44 M^{-1}cm^{-1}).

X-ray crystal structure of $[Cu(-)\text{-}L1](PF_6)_6\cdot(CH_3CN)_3\cdot(C_4H_{10}O)_{1.5}\cdot(H_2O)$: $[Cu(C_{42}H_{42}N_4)](PF_6)_6\cdot(CH_3CN)_3\cdot(C_4H_{10}O)_{1.5}\cdot(H_2O)$; M_r=5120; μ= 1.39 mm^{-1}, ρ_{calcd}=1.143 g cm^{-3}, hexagonal, $P6$, Z=1, a=26.894(4), c= 11.876(1) Å, V=7439(3) Å^3; extremely fragile hexagonal red prism, $0.40\times0.45\times0.52\times0.63$ mm, mounted on a quartz fiber with RS3000 oil. Cell dimensions and intensities were measured at 200 K on a Stoe Stadi4 diffractometer with graphite-monochromated $Cu_{K\alpha}$ radiation (λ= 1.5418 Å), $\omega-2\theta$ scans, scan width 1.08°+0.35 tg θ, and scan speed 0.075° s^{-1}. Two reference reflections measured every 45 min showed no variation. $0<h<24$; $0<k<24$; $0<l<12$ and all antireflections of these; 6461 measured reflections, 6093 unique reflections of which 4853 were observable ($|Fo|>4\sigma(F_0)$); R_{int} for 368 equivalent reflections=0.028. Data were corrected for Lorentz and polarization effects and for absorption (T_{min}=0.5349, T_{max}=0.6236). The compound is isostructural to the Ag complex.[11] All calculations were performed with the XTAL system[38] and ORTEP[39] programs. Definition of polar origin: z(Cu)=0.2 applied as a hard constraint. Flack parameter[40] x=0.10(7). Full-matrix least-squares refinement based on F by using a weight of $1/(\sigma^2(F_0)+0.002(F_0^2))$ gave final values of R=0.078, wR=0.094, and S= 2.33(4) for 580 variables and 4853 contributing reflections. The maximum shift/error on the last cycle was 0.39×10^{-3}. Hydrogen atoms of the complex were placed in calculated positions. The $Cu_6(-)\text{-}L1_6$ complex and PF_6 anion were refined with anisotropic displacement parameters. The PF_6 anion is disordered and twelve fluorine atomic sites have been observed and refined with population parameters of 0.5. The inclusion molecules of water (located on threefold and sixfold axes), acetonitrile, and diethyl ether show large disorders and partially occupied atomic sites and have been refined with isotropic displacement parameters without calculated hydrogen positions. These important disorders lead to a relatively poor diffraction, large overall displacement parameters, and high final values of R and uncertainties. The final difference electron density map showed a maximum of +0.79 and a minimum of −0.33 e Å^{-3}. The molecular packing shows compact layers of hexanuclear cationic complexes separated by layers containing the PF_6 anions and solvent molecules, a structure explaining the easy cleavage of the crystals along the (110) planes.

X-ray crystal structures of (+)-L1 and *meso*-L1: Intensity data were collected at 293 K on a Stoe Image Plate Diffraction System equipped with a ϕ circle, by using $Mo_{K\alpha}$ graphite-monochromated radiation (λ= 0.71073 Å) with a ϕ range of 0–200°, increments of 1°, 2θ range of 3.3–52.1°, and $D_{min}-D_{max}$ range of 12.45–0.81 Å .The structure was solved by direct methods by using the program SHELXS-97.[41] The refinement and all further calculations were carried out by using SHELXL-97.[42] Hydrogen atoms were included in calculated positions and treated as riding atoms by using the SHELXL-97 default parameters (AFIX 137 for the methyl hydrogen atoms). The non-hydrogen atoms were refined anisotropically by using weighted full-matrix least-squares refinement on F^2. The bond lengths and angles in the molecule are normal within experimental error. Details concerning data collection and refinement details are given in Table 1.

Acknowledgements

The authors thank F. Monlien and Prof. A. E. Merbach for the NMR measurements at low temperature, Dr. G. Hopfgartner, F. Nyddegger and H. Nierengarten for ES MS measurements. The Fond National Suisse de la Recherche Scientifique supported this project.

[1] C. Piguet, G. Hopfgartner, G. Bernardinelli, *Chem. Rev.* **1997**, *97*, 2005.
[2] M. Albrecht, *Chem. Rev.* **2001**, *101*, 3457.
[3] V. G. Machado, P. N. W. Baxter, J.-M. Lehn, *J. Braz. Chem. Soc.* **2001**, *12*, 431.
[4] R. Annunziata, M. Benaglia, M. Cinquini, F. Cozzi, C. R. Woods, J. S. Siegel, *Eur. J. Org. Chem.* **2001**, 173.
[5] M. Cantuel, G. Bernardinelli, G. Muller, J. P. Riehl, C. Piguet, *Inorg. Chem.* **2004**, *43*, 1840.
[6] J. Hamblin, L. J. Childs, N. W. Alcock, M. J. Hannon, *J. Chem. Soc. Dalton Trans.* **2002**, 164.
[7] A. Orita, T. Nakano, D. L. An, K. Tanikawa, K. Wakamatsu, J. Otera, *J. Am. Chem. Soc.* **2004**, *126*, 10389.
[8] R. Prabaharan, N. C. Fletcher, M. Nieuwenhuyzen, *J. Chem. Soc. Dalton Trans.* **2002**, 602.
[9] P. Hayoz, A. von Zelewsky, H. Stoeckli-Evans, *J. Am. Chem. Soc.* **1993**, *115*, 5111.
[10] H. Mürner, G. Hopfgartner, A. von Zelewsky, *Inorg. Chim. Acta* **1998**, *271*, 36.
[11] O. Mamula, A. von Zelewsky, G. Bernadinelli, *Angew. Chem.* **1998**, *110*, 301; *Angew. Chem. Int. Ed. Engl.* **1998**, *37*, 289.
[12] O. Mamula, A. von Zelewsky, T. Bark, G. Bernadinelli, *Angew. Chem.* **1999**, *111*, 3129; *Angew. Chem. Int. Ed.* **1999**, *38*, 2945.
[13] B. Kolp, D. Abeln, H. Stoeckli-Evans, A. von Zelewsky, *Eur. J. Inorg. Chem.* **2001**, 1207.
[14] O. Mamula, F. Monlien, A. Porquet, G. Hopfgartner, A. E. Merbach, A. von Zelewsky, *Chem. Eur. J.* **2001**, *7*, 533.
[15] J. Breu, H. Domel, A. Stoll, *Eur. J. Inorg. Chem.* **2000**, 2401.
[16] J. Breu, H. Domel, P.-O. Norrby, *Eur. J. Inorg. Chem.* **2000**, 2409.
[17] J. Breu, W. Seidl, D. Huttner, F. Kraus, *Chem. Eur. J.* **2002**, *8*, 4454.
[18] D. R. Desiraju, *The Crystal as a Supramolecular Entity*, Wiley, Chichester, **1996**.
[19] J. Jacques, A. Collet, *Enantiomers, Racemates, and Resolutions*, Wiley, New York, **1981**.
[20] J.-M. Lehn, *Supramolecular Chemistry—Concepts and Perspectives*, VCH, Weinheim, **1995**, Chapter 9.

[21] J.-M. Vincent, C. Philouze, I. Pianet, J.-B. Verlhac, *Chem. Eur. J.* **2000**, *6*, 3595.
[22] I. Pianet, J.-M. Vincent, *Inorg. Chem.* **2004**, *43*, 2947.
[23] M. A. Masood, E. J. Enemark, T. D. P. Stack, *Angew. Chem.* **1998**, *110*, 973; *Angew. Chem. Int. Ed.* **1998**, *37*, 928.
[24] J. M. Rowland, M. M. Olmstead, P. K. Mascharak, *Inorg. Chem.* **2002**, *41*, 1545.
[25] P. N. Taylor, H. L. Anderson, *J. Am. Chem. Soc.* **1999**, *121*, 11538.
[26] A. Wu, L. Isaacs, *J. Am. Chem. Soc.* **2003**, *125*, 4831.
[27] H.-J. Kim, D. Moon, M. S. Lah, *Angew. Chem.* **2002**, *114*, 3306; *Angew. Chem. Int. Ed.* **2002**, *41*, 3174.
[28] E. J. Enemark, T. D. P. Stack, *Angew. Chem.* **1998**, *110*, 977; *Angew. Chem. Int. Ed.* **1998**, *37*, 932.
[29] C. G. Claessens, T. Torres, *J. Am. Chem. Soc.* **2002**, *124*, 14522.
[30] T. W. Kim, M. S. Lah, J.-I. Hong, *Chem. Commun.* **2001**, 743.
[31] C. Provent, G. Bernadinelli, A. F. Williams, N. Vulliermet, *Eur. J. Inorg. Chem.* **2001**, 1963.
[32] a) D. A. Evans, M. C. Kozlowski, J. A. Murry, C. S. Burgey, K. R. Campos, B. T. Connell, R. J. Staples, *J. Am. Chem. Soc.* **1999**, *121*, 669; b) R. Noyori, S. Suga, K. Kawai, S. Okada, M. Kitamura, *Pure Appl. Chem.* **1988**, *60*, 1597; R. Noyori, M. Kitamura, *Angew. Chem.* **1991**, *103*, 34; *Angew. Chem. Int. Ed. Engl.* **1991**, *30*, 49.
[33] O. Maury, J. Lacour, H. Le Bozec, *Eur. J. Inorg. Chem.* **2001**, 201.
[34] T. Bark, M. Düggeli, H. Stoeckli-Evans, A. von Zelewsky, *Angew. Chem.* **2001**, *113*, 2924; *Angew. Chem. Int. Ed.* **2001**, *40*, 2848.
[35] R. A. Sheldon, *Chirotechnology*, Marcel–Dekker, New York, **1993**.
[36] D. B. Cline, *Physical Origin of Homochirality in Life*, AIP Press, Woodbury, NY, **1996**.
[37] G. J. Kubas, *Inorg. Synth.* **1979**, *17*, 90.
[38] S. R. Hall, H. D. Flack, J. M. Stewart, *XTAL3.2 User's Manual*, Universities of Western Australia and Maryland, **1992**.
[39] C. K. Johnson, *Ortep II*, Oak Ridge National Laboratory, Oak Ridge, TN, **1976**.
[40] H. D. Flack, *Acta Crystallogr. Sect. A* **1983**, *39*, 876.
[41] G. M. Sheldrick, *Acta Crystallogr. Sect. A* **1990**, *46*, 467.
[42] G. M. Sheldrick, SHELXL-97, Universität Göttingen, Göttingen, **1997**.

Received: November 3, 2004
Published online: March 15, 2005

